

## Effect of High Pressure on the Thermoelectric Power and Electrical Resistance of Aluminum and Gold\*

R. R. BOURASSA,† D. LAZARUS, AND D. A. BLACKBURN‡

*Department of Physics and Materials Research Laboratory, University of Illinois, Urbana, Illinois*

(Received 2 August 1967)

The effect of pressure up to 4 kbar on the thermoelectric power of aluminum, gold, nickel, and platinum has been determined. The change in resistance with pressure of aluminum and gold has also been measured. Measurements were carried out at temperatures between room temperature and 1300°K or, in the case of aluminum, between room temperature and 900°K. The high-temperature thermoelectric-power data for aluminum are separated into terms associated with three thermally activated defects: the monovacancy, the divancy, and the impurity-vacancy pair. Values for the formation energy and volume are obtained for each of these defects. The effect of vacancies in gold is dominated by the effect of pressure on the lattice so that no quantitative results can be determined. An effect consistent with a monovacancy model is detected. Measurements in platinum and nickel were carried out to test the sensitivity of the method to changes in scattering mechanism. A phenomenological model is presented to explain the resistance data in aluminum and gold. This model gives the accepted formation volume for monovacancies in gold. It gives a value for the formation volume of monovacancies in aluminum in agreement with the value obtained from thermoelectric-power measurements. The presence of divacancies in aluminum is strongly supported by this model.

### I. INTRODUCTION

#### A. Effect of Defects on the Thermoelectric Power of Metals

SINCE 1945 a great deal of experimental and theoretical work has been done on the thermoelectric power of metals. The conclusions are both discouraging and challenging. In a metal at absolute temperature  $T$  above the Debye temperature  $\theta_D$ , the thermoelectric power is given by

$$S = (\pi^2 k^2 T / 3 |e| \epsilon_F) [\partial \ln \rho(\epsilon) / \partial \ln \epsilon]_{\epsilon_F}, \quad (1)$$

where  $k$  is Boltzmann's constant,  $e$  is the electron charge, and  $\epsilon_F$  is the Fermi energy.<sup>1</sup> The term in the brackets is the logarithmic derivative of the resistivity with respect to the energy evaluated at the actual Fermi energy of the metal. The thermoelectric power is a direct measure of the energy dependence of the resistivity at the Fermi surface. Thus, thermoelectric power is more sensitive than the resistivity to the details of the scattering mechanism. The explanation of these details on the basis of models has proven difficult. The most notable problem is the lack of a model to explain the sign of the thermoelectric power in the noble metals.<sup>2</sup>

The application of thermoelectric-power measurements to the field of defect physics can be divided into two classes: experiments on dilute alloys and experiments on quenched metals. Mathiessen's rule holds approximately for low concentration of defects so that

$$S = (\pi^2 k^2 T / 3 |e| \epsilon_F) [\partial \ln(\rho_0 + \rho_i) / \partial \ln \epsilon]_{\epsilon_F}, \quad (2)$$

\* This work was supported in part by the U. S. Atomic Energy Commission under Contract No. AT(11-1)-1198.

† Present address: Battelle Memorial Institute, Richland, Wash.

‡ Present address: University of York, York, England.

<sup>1</sup> J. M. Ziman, *Electrons and Phonons* (Oxford University Press, London, 1960).

<sup>2</sup> F. J. Blatt, *Phys. Letters* **8**, 235 (1964).

where  $\rho_0$  is the lattice resistivity and  $\rho_i$  is the defect resistivity. Assuming that the Fermi energy is not changed, Eq. (2) becomes

$$S = S_0 + (S_i - S_0) \rho_i / \rho, \quad (3)$$

where

$$S_0 = (\pi^2 k^2 T / 3 |e| \epsilon_F) [\partial \ln \rho^0 / \partial \ln \epsilon]_{\epsilon_F}, \quad (4)$$

and

$$S_i = (\pi^2 k^2 T / 3 |e| \epsilon_F) [\partial \ln \rho_i / \partial \ln \epsilon]_{\epsilon_F}.$$

Equation (3) is called the Nordheim-Gorter relation. This relation can be applied directly in dilute alloys. A plot of the measured thermoelectric power  $S$  against the inverse of the measured total electrical resistivity ( $1/\rho$ ) should give a straight line.  $S_0$  and  $S_i$  can be obtained from the intercept and slope.

In quenching experiments the problems are complex. A sample, in the form of a wire, is heated to a temperature near the melting point so that the number of thermally activated defects in thermal equilibrium is large. The sample is then quenched, and the difference in thermoelectric emf between the quenched sample and a well-annealed sample is measured by forming a couple and applying a small temperature gradient. To avoid annealing the quenched defects, measurements must be made at low temperature where phonon drag is present. The large phonon-drag contribution to the thermoelectric power must be subtracted in order to use Eq. (3). There is also evidence that in some metals divacancies are formed during quenching. Equation (3) can be applied to quenching measurements by defining

$$\Delta S = S - S_0. \quad (5)$$

$S - S_0$  now represents the difference between the thermoelectric power of the quenched sample and the annealed sample,  $\rho_i/\rho$  is the ratio of the defect resistivity to the total resistivity of the quenched sample, and  $S_i$  is the intrinsic thermoelectric power of the defect as defined in Eq. (4). At a given temperature, for small defect

concentrations,  $\Delta S/\rho_i$  should be constant, since  $\rho$  does not change significantly with defect concentration. Huebener<sup>3,4</sup> has found values for gold and platinum of  $(\Delta S/C_v)_{200^\circ\text{K}} = -1.67 \mu\text{V}/^\circ\text{K}$  at.‰ and  $+2.6 \mu\text{V}/^\circ\text{K}$  at.‰, respectively, where  $C_v$  is the vacancy concentration.

### B. Pressure Effects on Thermoelectric Power: This Experiment

In the face-centered-cubic metals the predominant thermally activated defect is the monovacancy. This experiment was undertaken with the idea that the thermoelectric power of such a metal might be used as a tool to investigate vacancies at high temperatures. It was hoped that a small change in concentration of vacancies, brought about by the use of pressure, might produce a large effect through the measurement of the thermoelectric power which is very sensitive to any change in scattering mechanism. The advantage of this experiment over a quenching experiment is that the measurement can be made at high temperatures. This eliminates problems due to nonequilibrium and problems due to phonon drag. This method has its own problems, however. The vacancy concentration is not the only parameter that is changed. Pressure changes the lattice constant of the crystal and this in turn causes changes in the Fermi level. Pressure also changes the phonon-electron interaction and the phonon distribution itself. In this experiment an attempt is made to subtract these effects using low-temperature results as a base.

Bridgman<sup>5</sup> has measured the effect of pressure on the thermoelectric power of aluminum and gold as well as many other metals with pressures up to 12 kbar in the temperature range 0 to 100°C. This temperature range is far too low to see effects due to vacancies. The development of a pressure vessel able to withstand a pressure of 4 kbar at 1000°C in the present experiment permitted a considerable extension of the temperature range.

Dugdale and Mundy have measured the pressure dependence of the thermoelectric power of the alkali metals at room temperature.<sup>6</sup> They note that at high temperatures,  $T \geq \Theta_D$ , using the free-electron model,

$$d \ln S / d \ln V = \frac{2}{3}. \quad (6)$$

This relation is not confirmed by their experiments.

The fractional concentration of lattice vacancies in a metal in thermal equilibrium is given by

$$C_v = e^{-(\Delta U_F - T\Delta S_{\text{Th}} + P\Delta V_F)/kT}. \quad (7)$$

$\Delta U_F$ ,  $\Delta V_F$ , and  $\Delta S_{\text{Th}}$  represent the energy, volume, and entropy (excluding the entropy of mixing) associated with forming a lattice vacancy. The change in vacancy

concentration with pressure is given by

$$\partial \ln C_v / \partial P = -(1/kT)(-T\partial \Delta S_{\text{Th}} / \partial P + \partial \Delta U_F / \partial P + P\partial \Delta V_F / \partial P + \Delta V_F); \quad (8)$$

if it is assumed that the first three terms on the right are small compared to the fourth term, then

$$\partial \ln C_v / \partial P = -\Delta V_F / kT. \quad (9)$$

The first three terms cancel exactly if the entropy of mixing is included.

If we form a couple of a wire under pressure  $P_1$  and an identical wire under pressure  $P_2$ , the resulting difference in thermoelectric power is

$$\Delta S = S^{P_2} - S^{P_1}. \quad (10)$$

$S^P$  denotes the absolute thermoelectric power of the metal at pressure  $P$ . From Eq. (3)  $\Delta S$  can be written

$$\Delta S = [S_0 + (S_i - S_0)\rho_i/\rho]_{P_2} - [S_0 + (S_i - S_0)\rho_i/\rho]_{P_1}. \quad (11)$$

Then

$$\Delta S = (S_{0P_2} - S_{0P_1}) + \frac{\rho_i}{\rho} \left[ \frac{\Delta P \Delta V_F}{kT} (S_0 - S_i) + (S_{iP_2} S_{iP_1}) - (S_{0P_2} - S_{0P_1}) \right], \quad (12)$$

where  $\Delta P = P_2 - P_1$ . We have assumed that

$$\left( \frac{\rho_i}{\rho} \right)_{P_1} = \left( \frac{\rho_i}{\rho} \right)_{P_2}, \quad (13)$$

where  $\rho_i = \rho_i 1\% C_v$ , and we have used the expansion

$$e^{-\Delta P \Delta V_F / kT} \simeq 1 - \Delta P \Delta V_F / kT. \quad (14)$$

This simple model clearly shows the expected temperature dependence of  $\Delta S$ .

$$\Delta S = \Delta S_0(T) + e^{-\Delta U_F / kT} f(T), \quad (15)$$

where  $\Delta S_0$  and  $f$  are slowly varying functions of temperature. We have assumed that  $P_1 \Delta V_F \ll \Delta U_F$ . The sign of  $f(T)$  can be positive or negative. We can write

$$f e^{-\Delta U_F / kT} \simeq \frac{\rho_i}{\rho} \frac{\Delta P \Delta V_F}{kT} (S_0 - S_i). \quad (16)$$

Define

$$\delta S \equiv S - S_0 = (\rho_i/\rho)(S_i - S_0) \quad (17)$$

from Eq. (5). Since  $P_1 \Delta V_F \ll \Delta U_F$ ,

$$C_v = 100 e^{\Delta S_{\text{Th}} / k} e^{-\Delta U_F / kT} \text{ at.}\% \quad (18)$$

Thus,

$$f = -(\delta S/C)(\Delta P \Delta V_F / kT) e^{\Delta S_{\text{Th}} / k}. \quad (19)$$

From Huebener's data on gold,

$$(\delta S/C)_{200^\circ\text{K}} = -1.67 \mu\text{V}/^\circ\text{K} \text{ at.}\% \quad (20)$$

This value should be nearly independent of tempera-

<sup>3</sup> R. P. Huebener, Phys. Rev. **135**, A1281 (1964).

<sup>4</sup> R. P. Huebener, Phys. Rev. **146**, 490 (1966).

<sup>5</sup> P. W. Bridgman, Proc. Am. Acad. Arts Sci. **53**, 269 (1918).

<sup>6</sup> J. S. Dugdale and J. N. Mundy, Phil. Mag. **6**, 1463 (1961).

ture. If we assume that

$$|\delta S/C|_{Al} = |\delta S/C|_{Au}, \quad (21)$$

the effect of vacancies on the change in thermoelectric power of Al with pressure can be estimated. Define  $\Delta S_i$  as the change in thermoelectric power due to vacancies such that

$$\Delta S = \Delta S_0 + \Delta S_i. \quad (22)$$

Then,

$$\Delta S_i = f e^{-\Delta U_F/kT}. \quad (23)$$

We take  $(\Delta S_{Th}/k)_{Al} = 2.4$ ,  $(\Delta S_{Th}/k)_{Au} = 1.0$ ,  $(\Delta U_F)_{Al} = 0.77$  eV, and  $(\Delta U_F)_{Au} = 0.94$  eV from the work of Simmons and Balluffi.<sup>7,8</sup> For  $\Delta P = 4$  kbar and  $\Delta V_F = 10^{-23}$  cm<sup>3</sup> we find

$$\begin{aligned} \Delta S_i_{Au}(1323^\circ\text{K}) &= 0.017 \mu\text{V}/^\circ\text{K}, \\ \Delta S_i_{Al}(923^\circ\text{K}) &= |0.038| \mu\text{V}/^\circ\text{K}. \end{aligned} \quad (24)$$

The method used in this experiment can easily detect changes of this order.

In order to test the sensitivity of the method to changes in scattering mechanism the experiment was also carried out on platinum and nickel samples. Nickel was chosen because of the known change in scattering mechanism which occurs at the Curie temperature. Platinum was chosen because no change in scattering mechanism is expected to occur in the temperature range 300 to 1300°K. The temperature range is too low to see vacancy effects in either platinum or nickel.

The difference between the thermoelectric power of one side of a couple and that of the other is given by the temperature derivative of the emf of the couple. In this experiment the emf was measured as a continuous function of temperature while the pressure was held constant, to provide optimal data for determination of the derivatives.

### C. Pressure Effects on Resistance: This Experiment

Bridgman has measured the effect of pressure on resistance of Al and Au along with many other materials in the temperature range 0 to 100°C.<sup>9</sup> The development of the present pressure vessel has permitted extending the temperature range to 1000°C.

In this part of the experiment the change in resistance with pressure was measured while the temperature was held constant. In the measurement of thermoelectric emf the change with temperature was measured while the pressure was held constant.

## II. EXPERIMENTAL EQUIPMENT AND PROCEDURES

The present experiment involved measurement of extremely small changes in thermoelectric power and

electrical resistivity, so a null method was essential. Changes in thermoelectric emf were determined by balancing the output of a junction under hydrostatic pressure against an identical junction without pressure. A similar balanced arrangement was needed for measurement of resistance changes. Although the pressure-induced changes in thermoelectric power and resistance were small, the thermoelectric voltages and bridge voltages were large and, of course, strongly temperature-dependent. For this reason, it was essential that fluctuating thermal gradients be eliminated.

Ordinary high-pressure-high-temperature techniques, involving furnaces internal to the pressure vessel, were clearly inadequate. Temperature fluctuations due to convection in the pressure gas and from inherent imbalance between the specimen and "dummy" furnaces would have completely obscured the pressure-induced changes in thermoelectric power and resistivity. To minimize fluctuations in the thermal gradient, a completely symmetrical system was employed. Both specimen and "dummy" wires were enclosed within a single massive externally heated bar of metal with identical external fittings and lead-in wires. Either half of the metal bar could be pressurized. Thus the pressure vessel and furnace were combined as a single unit.

### A. Pressure Vessel

The pressure vessel was made from a 1½-in.-diam, 42-in.-long bar of Moly TZM<sup>10</sup> alloy. Axial holes 5/8 in. in diam were drilled from each end, leaving a solid bridge of metal ½ in. in thickness at the center. TZM alloy was chosen because it will withstand pressures of at least 4 kbar at temperatures ranging from 300 to 1300°K. The maximum pressure was restricted to 4 kbar since higher pressures would reduce the working lifetime of the vessel and enhance the probability of pinchoff of wires in pressure seals. A pressure of 4 kbar produced changes in thermal voltages which were easily measurable. Heater windings were wrapped directly around the central 29 in. of the bar over a 1/16 in. layer of Refrasil cloth. A 10-Ω platinum resistance thermometer encased in ceramic was placed directly on the windings over the center of the pressure vessel. Two 1/16 in. layers of Refrasil cloth covered the windings and resistance thermometer. Refrasil thread held the cloth in place, and Refrasil tape completed the insulation. The windings were of No. 22 nicrome wire and were spaced 5 turns per in. The maximum temperature gradient across the center of the pressure vessel was 1/3 K° at 1300°K. The temperature of the ends of the bar was held constant by a temperature-controlled water-cooling system. A water-cooling jacket also surrounded the body of the vessel.

The ends of the pressure vessel were ground flat and threaded. An O-ring pressure seal was made between

<sup>7</sup> R. O. Simmons and R. W. Balluffi, *Phys. Rev.* **117**, 52 (1960).

<sup>8</sup> R. O. Simmons and R. W. Balluffi, *Phys. Rev.* **125**, 862 (1962).

<sup>9</sup> P. W. Bridgman, *Proc. Am. Acad. Arts Sci.* **52**, 573 (1917).

<sup>10</sup> Climax Molybdenum Co., Detroit, Mich.

the flat end of the bar and the flat on the threaded end of a five-way coupling described below. The two pieces were joined by a conventional gland-nut arrangement. This assembly is shown in Fig. 1.

The five-way coupling was made of heat-treated 4340 steel. Four openings were fitted for  $\frac{5}{16}$ -in. o.d. pressure tubing. The fifth opening allowed access to the  $\frac{1}{2}$ -in.-diam,  $\frac{1}{2}$ -in.-long cylindrical working chamber and was sealed by a conventional Bridgman seal.

### B. Pressure-Couple Circuit

The samples were of 0.010-in.-diam wire. Aluminum wire of 99.9999% purity was obtained from Cominco American Inc., Spokane, Wash. Sigmund Cohn of Mount Vernon, N. Y., supplied the nominally 99.999% pure gold wire. The nickel and platinum wires were supplied by A. D. Mackay, New York, and were nominally 99.9% pure. The wire was inserted through one of the 4 holes in a 25-in.-long,  $\frac{1}{8}$ -in.-diam AP35 alumina insulating tube obtained from McDanel Refractory Porcelain Co. A few inches of the wire were looped back into one of the remaining holes. The ceramic tube was inserted in the pressure vessel, and electrical contact was made between the metal wire and the center of the pressure vessel by forcing the tube against the center with a spring mounted in the five-way coupling. At the cold end, the wire was insulated with 0.027-in.-o.d. Teflon tubing. This insulation originated a few inches inside the ceramic tube so that short circuits in the five-way coupling were avoidable. The insulated wire was brought out of the five-way coupling through  $\frac{5}{16}$ -in.-o.d. pressure tubing. This tubing formed a "U" and was filled with oil. Liquid nitrogen was used to freeze this oil, forming a pressure seal and the cold junction of the pressure couple. Outside the pressure seal, the wire was threaded through copper tubing to the measuring system to eliminate emf's produced by air drafts and changing magnetic fields. At two positions along the wire, outside the pressure system, connections

were made in thermal-free junction boxes. Both specimen and dummy circuits were identical, mechanically and electrically. The junction between the two sides of the circuit and the center of the pressure vessel formed the hot junction of the pressure couple. Without elevated pressure or temperature, the thermal emf's in this circuit for aluminum were never more than 0.03  $\mu\text{V}$  and usually were 0.00 to 0.01  $\mu\text{V}$ .

A Chromel-Alumel thermocouple was inserted into the vessel through the remaining two holes in the ceramic tube. The temperature was measured at a point less than  $\frac{1}{8}$  in. away from the hot junction of the pressure couple. At a point 3 in. away, the temperature differed by less than 1 K° so that any error in the temperature reading was due entirely to the calibration. The thermocouple was brought out through another frozen-oil pressure seal. Connections were made in an ice bath to copper wires forming the cold junction of the thermocouple.

### C. Measuring System

A Honeywell model 2768 six-dial potentiometer was used to measure the emf of the pressure couple for the thermoelectric-power measurements. The galvanometer and amplifier system was a Honeywell model 3550 photoelectric galvanometer for the measurements on aluminum and a Leeds and Northrup model 9835 dc amplifier for measurements on the other metals. Measurements were made with the potentiometer unbalanced. This signal was amplified and recorded, together with the Chromel-Alumel thermocouple voltage, on a Mosely two-pen strip chart recorder. The maximum change in thermoelectric emf in the aluminum measurements was less than 5  $\mu\text{V}$ , and in this range the photoelectric galvanometer is linear. This linearity was checked every few runs, and a calibration was established. Corrections were less than  $\pm 0.05 \mu\text{V}$ . Voltages produced in the gold, nickel, and platinum couples exceeded 5  $\mu\text{V}$  and the corrections became significant. Because it is linear

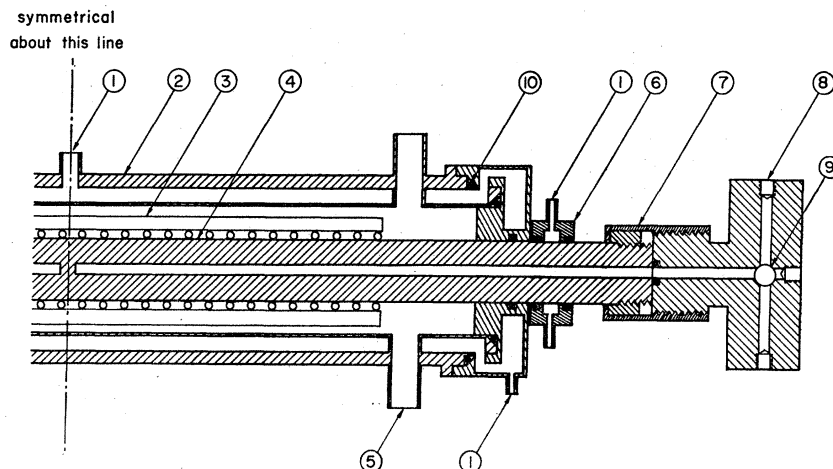


FIG. 1. Assembly of pressure vessel, furnace, and five-way coupling: (1) water inlet; (2) water jacket; (3) furnace; (4) pressure vessel; (5) power lead exit; (6) watercooling end block; (7) conventional gland-nut arrangement; (8) five-way coupling; (9)  $\frac{1}{2}$ -in.-cylindrical working chamber with Bridgman seal fitting; (10) o-rings.

in the range 0 to 2000  $\mu\text{V}$ , the dc amplifier eliminated these corrections. This amplifier was not suitable for the aluminum measurements because readings in the 0–5- $\mu\text{V}$  range would include an inherent error of  $\pm 0.2 \mu\text{V}$ .

#### D. Pumping Station

Pressure was applied to one side of the pressure couple; the other side was maintained at 0.1 kbar, using argon gas. To provide an inert atmosphere, the volume between the TZM bar and the water jacket was filled with argon gas. The pumping station was essentially the same as that described by Fitchen.<sup>11</sup> An air-driven pump pressurized an oil-gas separator to 2 kbar. The 2-kbar argon gas was used to fill the high-pressure side of a 15:1 Harwood intensifier, which brought the vessel and a ballast volume to the desired pressure. A General Electric model LC10 helium leak detector was used to find small gas leaks anywhere in the pressure system. A small amount of helium was added to the argon gas in order to detect these leaks. Pressure variations over a period of eight h were less than 7 bar as measured on a Heise 100 000 psi gauge. The ballast volume allowed this variation to be maintained while the temperature of the hot junction was varied by 1000 K°.

It was important that no temperature gradient exist across the pressure junction formed by the frozen-oil seal. Such gradients were eliminated by raising the liquid N<sub>2</sub> level after the application of pressure, insuring the immersion of the pressure junction in a constant temperature bath. If this was not done, the pressure junction was formed near the liquid N<sub>2</sub> level where a large temperature gradient existed. Care was taken to maintain the liquid N<sub>2</sub> level above the pressure junction throughout fixed pressure measurements.

Cold traps in the gas-pressure line, maintained at the temperature of dry ice, insured that a minimum of contaminants reached the samples. The residual resistance ratio ( $R_{300^\circ\text{K}}/R_{4.2^\circ\text{K}}$ ) of the aluminum samples

was 2000 before the runs, indicating an initial purity less than the 99.9999% stated by the manufacturer. Lack of contamination was indicated by a post-run ratio of 1800.

#### E. Thermoelectric emf Measurement Procedure

The temperature of the hot junction was raised to 900°K for aluminum and to 1300°K for the other metals. This rise was automated, as described below, and took from 4 to 5 h. Measurements were taken during this rise and during the descent while the pressure was held constant. Figure 2 shows a reproduction of a recorder tracing of the change in thermoelectric emf and of the temperature of the hot junction. The zero and the linearity of the galvanometer were checked periodically; these checks also can be seen in Fig. 2.

Preceding the runs, the temperature and pressure were cycled to reduce cold-work effects. Several runs with zero pressure gradient were made before pressure runs were attempted so that a reproducible base emf could be established. This zero-pressure run was repeated after every pressure run. Once the wires had been annealed, the zero-pressure runs were reproducible.

Power was supplied to the furnace windings by a 220-V ac supply. The temperature control unit was a RT3R/MK2 fully proportional temperature controller obtained from Associated Electrical Industries. It operated in conjunction with a platinum resistance thermometer of 10  $\Omega$  as the temperature sensor. During constant temperature runs, this control unit maintained the temperature at the thermocouple to within  $\pm \frac{1}{2}$  K° in the range of 300 to 1300°K. During constant pressure runs, the temperature was raised or lowered by slowly changing the control setting by means of a synchronous motor and reduction gear drive. Typically, the temperature was raised from 300 to 1300°K in 5 h.

#### F. Resistance Measurement Procedure

The same vessel, furnace, and measuring system were used for the resistance measurements of aluminum and

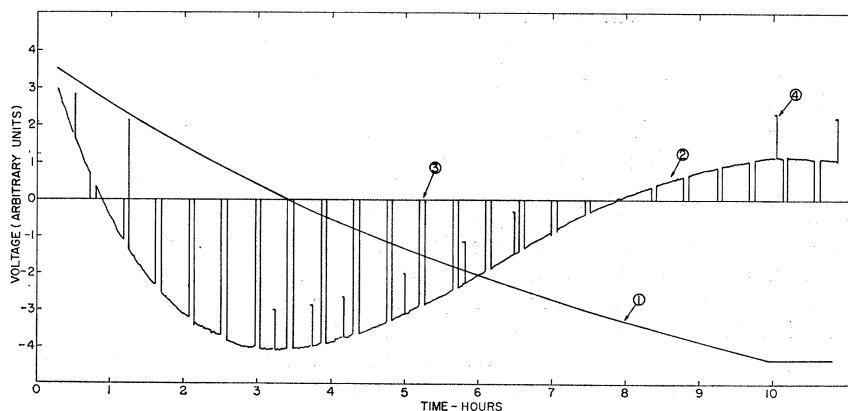


FIG. 2. Reproduction of recorder tracing: (1) trace of temperature versus time; (2) trace of the change in thermoelectric emf with pressure for aluminum for a pressure of 4.11 kbar; (3) a check on the galvanometer zero; (4) calibration mark.

<sup>11</sup> D. B. Fitchen, Rev. Sci. Instr. 34, 673 (1963).

gold. Measurements were made for 8 fixed temperatures at 5000-psi pressure intervals. A six-hole ceramic tube was used to insulate the two current leads, the two potential leads, and the two thermocouple leads. The potential leads and the current leads were taken from the same spool as the wire used in the thermoelectric emf measurements.

Resistance measurements were made using a differential technique, and reversing the current and repeating the measurements eliminated the effects of thermal emf's. The small temperature gradient across the center of the pressure vessel was assumed constant during the 1- to 2-h runs. Reproducibility of the data validated this assumption. Pressure effects on the temperature gradient due to changes in the thermal conductivity of argon under pressure were estimated and were found to be negligible. The effect of a temperature change at the ends of the vessel was not negligible, resulting in a  $0.04\text{-}\mu\text{V}$  change in unbalance voltage per degree change in temperature difference of the ends. This temperature difference was controlled to within  $\pm\frac{1}{2}\text{K}^\circ$  by the temperature-regulated water jacket described previously.

### G. Discussion of Experimental Accuracy

The main sources of error in this experiment arise from fluctuations in the temperature gradient across the center of the pressure vessel and the inherent instabilities of the measuring system.

In the thermoelectric-power measurements, zero pressure runs were made to determine the emf produced by the temperature gradient across the center of the pressure vessel. This emf was subtracted from the actual emf measured during a pressure run. The zero-pressure emf was 50% of the 1-kbar emf and 10% of the 4-kbar emf. Due to changes in the characteristics of the furnace, the magnitude of the slope of the zero-pressure emf could change by a maximum of 20%. The estimated error in the change in thermoelectric power due to changes in the temperature gradient across the center of the pressure vessel is 10% of the maximum  $\Delta S$  at 1 kbar and 2% of the maximum  $\Delta S$  at 4 kbar. Systematic errors due to inherent instability in the amplifier systems are estimated to be 2% of the maximum change in thermoelectric power. The absolute temperature in this experiment was measured with a calibrated Chromel-Alumel thermocouple, and an error in the temperature reading of  $\pm 1\text{K}^\circ$  is estimated.

Errors due to changing thermal emf's caused by drafts and stray magnetic fields were negligible in this experiment due to careful shielding of wires. Errors due to a temperature gradient across the low-temperature pressure junction were eliminated by immersing that junction in a constant temperature bath of liquid nitrogen. In the resistance measurements, null readings were used exclusively so that the error due to the measuring system was small compared to errors introduced due to changes in the temperature gradient across

the center of the pressure vessel. The change in that gradient throughout the 1- to 2-h extent of a resistance run is estimated at 5%. This estimate is based on the reproducibility of the zero pressure readings before and after a run. A 5% change in gradient produces an error of no more than 5% in the change in resistance due to pressure. The other major source of error is due to cold working, and this was reduced by annealing and pressure cycling of the specimen and dummy before measurements were begun. The reproducibility of the data indicates that errors from this source are no more than 5% of the maximum  $\Delta R$ .

## III. RESULTS AND DISCUSSION

A typical chart recording of the emf of the pressure couple and of the temperature of the hot junction is shown in Fig. 2. These strip charts were placed on 35-mm film and the data were digitized onto IBM cards by a Hydel model 200-A3 film reader. An IBM 7094 computer was programmed to analyze the data by a least-squares technique and to plot results.

### A. Discussion of Thermoelectric Power Data: Aluminum

The temperature derivative of the thermoelectric emf of a pressure couple is the difference in thermoelectric power of the two sides. The change with pressure of the thermoelectric power of Al as a function of temperature is shown in Fig. 3.

The change in thermoelectric power with pressure for aluminum changes sign in our temperature range near  $668^\circ\text{K}$ . To first order this temperature is independent of

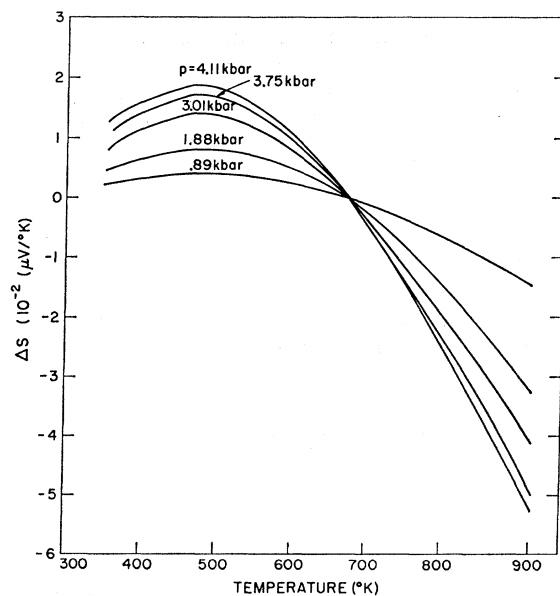


FIG. 3. Change in thermoelectric power with pressure as a function of temperature for aluminum.

pressure. This is a clear indication of the accuracy of the data since an error of 5% of the maximum  $\Delta S$  could introduce a spread of 75 K° in the temperature at which  $\Delta S$  crosses zero. Physically, this change in sign must reflect a change in scattering mechanism of one side of the couple relative to the other.

The maximum value of  $\Delta S$  at 4 kbar is  $0.05 \mu\text{V}/^\circ\text{K}$ . Our previous estimate of the effect due to vacancies was  $|\Delta S_i| = 0.038 \mu\text{V}/^\circ\text{K}$ . Thus, one would expect that in the case of aluminum an extrapolation of the low-temperature values of  $\Delta S$  would separate out the effects of vacancies. The extrapolation used in this analysis to determine  $\Delta S_i$  is indicated in Fig. 4 for a pressure of 4.11 kbar. The extrapolation is a linear extension of the data between  $T = 305^\circ\text{K}$  and  $T = 475^\circ\text{K}$ . Isotherms of  $\Delta S_i$  as a function of pressure indicate that  $\Delta S_i$  is linear

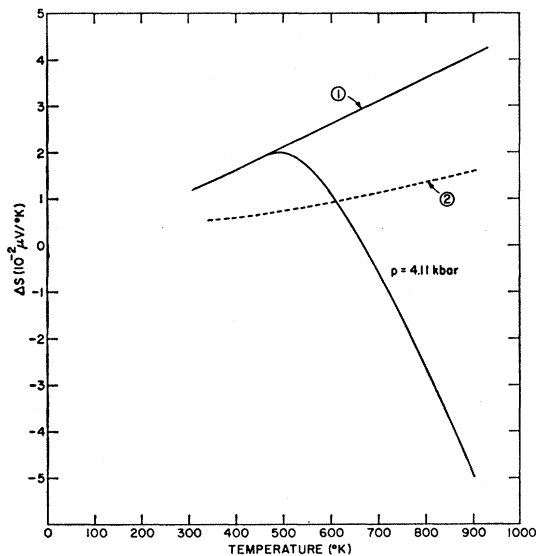


FIG. 4. Extrapolation of the change in thermoelectric power at low temperature: (1) linear extension of low-temperature data; (2) the change in thermoelectric power  $\Delta S_{\text{FEM}}$  calculated using the free-electron model.

in the pressure for all temperatures, in complete agreement with Eq. (19).

A linear extrapolation was chosen after an examination of the change in thermoelectric power with pressure exclusive of the effects due to thermally activated defects.

We expect as a first approximation that only the Fermi energy is changing due to the pressure. If we expand  $\Delta S$  in a Taylor series in the volume of the crystal and keep only the first term,

$$\Delta S = \Delta V (\partial S / \partial V)_{V_0}, \quad (25)$$

where  $\Delta V = V - V_0$ ,  $V$  is the volume under pressure,  $V_0$  is the volume of the unstressed crystal, and  $S$  is the absolute thermoelectric power of the metal. Equation

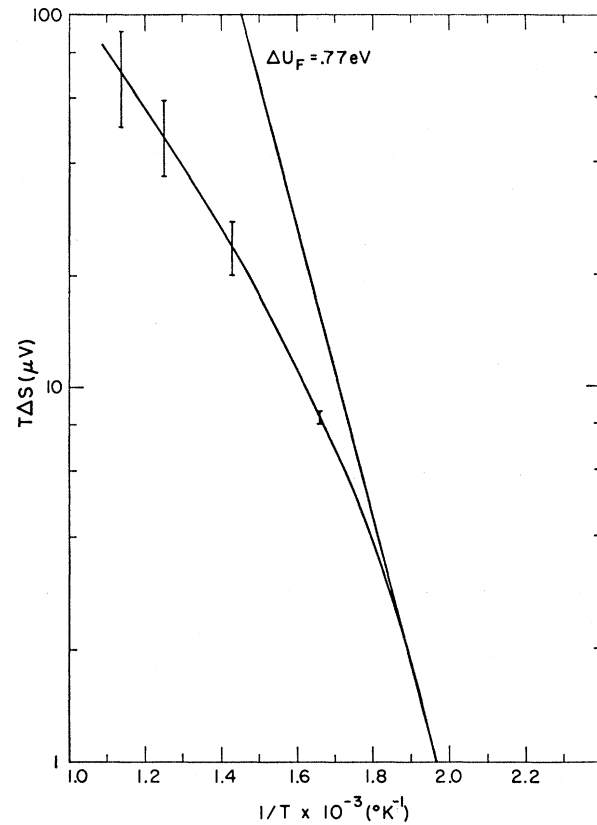


FIG. 5. Comparison of the change in thermoelectric power due to defects with a simple model.

(25) can be written, assuming the free-electron model,

$$\Delta S = S \chi \Delta P (\partial \ln S / \partial \ln V) = -\frac{2}{3} S \chi \Delta P, \quad (26)$$

where  $\chi$  is the isothermal compressibility. This value of  $\Delta S$  is denoted by  $\Delta S_{\text{FEM}}$  (FEM for free electron model).  $\Delta S_{\text{FEM}}$  is indicated in Fig. 4 by a dotted curve. The extrapolated curve is proportional to the free-electron curve,

$$\Delta S_{\text{extrapolation}} = 2.78 \Delta S_{\text{FEM}}, \quad (27)$$

indicating that

$$\partial \ln S / \partial \ln V = 1.85. \quad (28)$$

According to the assumption in our model, the difference between the actual change in thermoelectric power and the extrapolated curve should be  $\Delta S_i$ , the thermoelectric power due to the difference in concentration of vacancies between the two sides of the pressure couple. From Eq. (23), the logarithmic derivative of  $T\Delta S_i$  with respect to  $1/T$  should then be given by

$$\frac{\partial \ln T\Delta S_i}{\partial (1/T)} = -\frac{\Delta U_F}{k} (\text{K}^\circ). \quad (29)$$

The value for  $\ln T\Delta S_i$  obtained from the 4.11-kbar data is shown versus  $1/T$  in Fig. 5. The effect of other

extrapolations is indicated by the error bars and is, of course, large at high temperatures. Also shown in Fig. 5 is the slope representing the Simmons and Balluffi value of  $\Delta U_F \approx 0.77$  eV. The low-temperature segment of this curve agrees remarkably well with this value. It is clear, however, that the entire effect is not due to monovacancies unless the formation energy were highly temperature-dependent.

We may reexamine the model presented in Sec. I.B, now supposing that other defects are present in addition to the monovacancy. The arguments leading to Eq. (15) hold for any thermally activated defect, so that in general

$$\Delta S = \Delta S_0(T) + \sum_j (g_j/T) e^{-\Delta U_F^j/kT}, \quad (30)$$

where  $\Delta U_F^j$  is the formation energy of the  $j$ th type of defect.

$$g^j = 100(\delta S/C)^j (\Delta P \Delta V_F^j/k) e^{\Delta S_{Th}^j/k} \equiv f^j(T)/T, \quad (31)$$

where  $(\delta S/C)^j$ ,  $\Delta V_F^j$ , and  $\Delta S_{Th}^j$  are now defined for the  $j$ th-type defect. The approximation that  $\Delta P \Delta V_F/kT < 1$  is no longer valid since a divacancy might have twice the formation volume of a single vacancy. Equation (30) should then be written

$$\Delta S = \Delta S_0(T) + \sum_j^n A_j e^{-\Delta U_F^j/kT} (e^{-\Delta P \Delta V_F^j/kT} - 1), \quad (32)$$

where  $\Delta V_F$  is the formation volume of the  $j$ th type of defect.  $A_j$  is given by

$$A_j = 100(\delta S/C)^j e^{\Delta S_{Th}^j/k}. \quad (33)$$

Equation (32) was used to fit the data of seven pressure runs using 44 data points per run. Table I shows the results for  $n=1, 2$ , and 3, and the fit is indicated in Fig. 6 for  $\Delta P=4.11$  kbar. For  $n=3$  the curve predicted by the model is within the experimental error of the data and fits very well in the intermediate temperature range from 520 to 750°K. At temperatures higher than 750°K our extrapolation may introduce significant error, and at temperatures below 520°K  $\Delta S$  is too small to determine accurately.  $\Delta S$  obtained from Eq. (32) using  $n=1$  or  $n=2$  does not fit the data in the intermediate temperature range. A very plausible physical interpretation of the data emerges by considering the  $n=3$  solution to Eq. (32).

We easily recognize the term associated with monovacancies

$$\Delta S_1 = 1.5 \times 10^5 e^{-0.74 \text{ eV}/kT} (e^{-\Delta P \cdot 0.9 \times 10^{-23} \text{ cm}^3/kT} - 1). \quad (34)$$

This term indicates that

$$\Delta U_F^1 = 0.74 \text{ eV}, \quad (35)$$

and

$$\Delta V_F^1 = 0.9 \times 10^{-23} \text{ cm}^3. \quad (36)$$

This value for the formation volume is consistent with

the large activation volume found by Butcher, Hutto, and Ruoff.<sup>12</sup> Recent work by Bass<sup>13</sup> indicates a value for  $\Delta U_F^1$  of  $0.73 \pm 0.03$  eV. The value of  $A_1$  is very sensitive to changes in  $\Delta U_F$  and  $\Delta V_F$  and will give an order of magnitude estimate of  $\delta S/C$ . Using a formation entropy  $\Delta S_{Th}/k$  of 2.4 from Simmons and Balluffi,<sup>7</sup> we obtain

$$\delta S/C \approx 130 \mu\text{V}/^\circ\text{K at } 0\%. \quad (37)$$

This value for the specific vacancy contribution to the thermoelectric power seems large, but is consistent with the large effect observed for aluminum. However, it should be remembered that this value for  $\delta S/C$  is derived from one of the pre-exponential terms ( $A_1$  in Table I) in a fit which involves six exponential parameters and two other pre-exponential terms, so no undue emphasis should be placed on the actual value derived. Small variations in the other parameters can effect a change in  $\delta S/C$  by an order of magnitude.

We associate the second term

$$\Delta S_2 = -3.8 \times 10^4 e^{-0.64 \text{ eV}/kT} (e^{-\Delta P \cdot 0.6 \times 10^{-23} \text{ cm}^3/kT} - 1), \quad (38)$$

with an impurity-vacancy complex. The concentration of impurity-vacancy pairs is

$$C_{iv} = 12C_i C_v e^{B_{iv}/kT} = 12C_i e^{-\Delta U_F^1 - B_{iv}/kT}, \quad (39)$$

where  $C_i$  is the impurity concentration and  $B_{iv}$  is the impurity-vacancy binding energy. The value indicated for  $B_{iv}$  is

$$B_{iv} = 0.1 \text{ eV}. \quad (40)$$

The formation volume associated with the bound vacancy is then

$$\Delta V_{iv} = 0.6 \times 10^{-23} \text{ cm}^3. \quad (41)$$

This value is significantly less than the value found for the free monovacancy, indicating a relatively smaller expansion of the lattice when a vacancy is formed in the already strained region about an impurity atom. In order to estimate  $\delta S/C$  for impurity-vacancy pairs we would need to know the formation entropy and the concentration of defects in our wire. From our residual resistance measurements we find  $C_i \approx 10^{-4} - 10^{-5}$ . Other experiments would not have detected the impurity-vacancy complex due to the small concentration of such complexes at high temperatures. It is detected in this experiment because  $(\delta S/C)_{iv}$  enters with opposite sign compared to the monovacancy.

The third term in  $\Delta S$  may well be due to the divacancy.

$$\Delta S_3 = -3.3 \times 10^5 e^{-0.91 \text{ eV}/kT} (e^{-\Delta P \cdot 1.6 \times 10^{-23} \text{ cm}^3/kT} - 1). \quad (42)$$

This implies that

$$\Delta U_F^2 = 0.91 \text{ eV}, \quad (43)$$

and, since

$$\Delta U_F^2 = 2\Delta U_F^1 - B_2, \quad (44)$$

<sup>12</sup> B. M. Butcher, H. Hutto, and A. L. Ruoff, Appl. Phys. Letters 7, 34 (1965).

<sup>13</sup> J. Bass, Phil. Mag. 15, 717 (1967).



TABLE I. Results of a least-squares fit of measured values of the change in thermoelectric power of aluminum with temperature and pressure using one-, two-, and three-defect models.

$n$	$\Delta S = \Delta S_0(T) + \sum_j^n \Delta S_j$						$A_1$ ( $\mu\text{V}/^\circ\text{K}$ )	$A_2$ ( $\mu\text{V}/^\circ\text{K}$ )	$A_3$ ( $\mu\text{V}/^\circ\text{K}$ )
	$\Delta U_{F^1}$ (eV)	$\Delta U_{F^2}$ (eV)	$\Delta U_{F^3}$ (eV)	$\Delta V_{F^1}$ ( $10^{-23} \text{ cm}^3$ )	$\Delta V_{F^2}$ ( $10^{-23} \text{ cm}^3$ )	$\Delta V_{F^3}$ ( $10^{-23} \text{ cm}^3$ )			
1	0.44	...	...	5.0	...	...	40	...	...
2	0.60	0.59	...	0.83	0.82	...	$7.8 \times 10^6$	$-7.4 \times 10^6$	...
3	0.74	0.64	0.91	0.90	0.60	1.6	$1.5 \times 10^6$	$-3.8 \times 10^4$	$-3.2 \times 10^6$

that

$$B_2 = 0.57 \text{ eV}, \quad (45)$$

where  $B_2$  is the binding energy of a divacancy.

Doyama and Koehler<sup>14</sup> have reported evidence of two vacancy defects in quenched aluminum; and, by assuming that they are the monovacancy and the divacancy, they estimate that

$$B_2 = 0.17 \pm 0.5 \text{ eV}. \quad (46)$$

A binding energy of 0.57 would imply that the divacancy is an important defect in aluminum at high temperatures. There is no direct evidence contradicting this conclusion. Butcher, Hutto, and Ruoff<sup>12</sup> have measured the activation volume for self-diffusion in Al and find  $\Delta V_{\text{self-diffusion}} = 2.2 \times 10^{-23} \text{ cm}^3$ . This is the only example of a vacancy activation volume which is greater than an atomic volume. They offer two possible explanations for this unusually high volume: (1) The second nearest neighbor lies in a region of repulsive force so that extraction of an atom would result in an over-all expansion of the lattice; (2) the dominant equilibrium defect in aluminum is the divacancy. From the present result the formation volume  $\Delta V_{F^2}$  of the divacancy is  $1.6 \times 10^{-23} \text{ cm}^3$ , slightly less than twice that of the isolated monovacancy.

The experiments of Simmons and Balluffi<sup>7,8</sup> measure only the total net defect concentration and so cannot directly distinguish between types of vacancies. A least squares fit was made to the data of Simmons and Balluffi<sup>7</sup> assuming formation energies  $\Delta U_{F^1} = 0.74 \text{ eV}$  and  $\Delta U_{F^2} = 0.91 \text{ eV}$ . The formation entropies of the single vacancy and of the divacancy were varied. The best fit was obtained for  $\Delta S_{F^1}/k = 1.6$ , and  $\Delta S_{F^2}/k = 1.1$ . This would imply that the formation entropy of a divacancy is not simply double that of a single vacancy.

It is currently believed that in many metals divacancies form during quenching so that data taken from such experiments may be interpretable in terms of divacancies rather than monovacancies.

## B. Discussion of Thermoelectric-Power Data: Gold

Figure 7 shows the change in the thermoelectric power of gold with pressure as a function of tempera-

<sup>14</sup> M. Doyama and J. S. Koehler, Phys. Rev. **134**, A522 (1964).

ture. The maximum value of  $\Delta S$  at 4 kbar is  $0.1 \mu\text{V}/^\circ\text{K}$ . The estimate of  $\Delta S_i$  of  $0.017 \mu\text{V}/^\circ\text{K}$  indicates that a vacancy effect should be large enough to be observed but too small to expect accuracy from an extrapolation method.

The change in thermoelectric power due to vacancies,  $\Delta S_i$ , was calculated from Eqs. (19) and (23) with no adjustable parameters. The calculated  $\Delta S_i$ 's were subtracted from the measured values. The residual represents the change in thermoelectric power due to pressure caused by parameters other than the concentration of vacancies. The residuals are shown as a dotted curve in

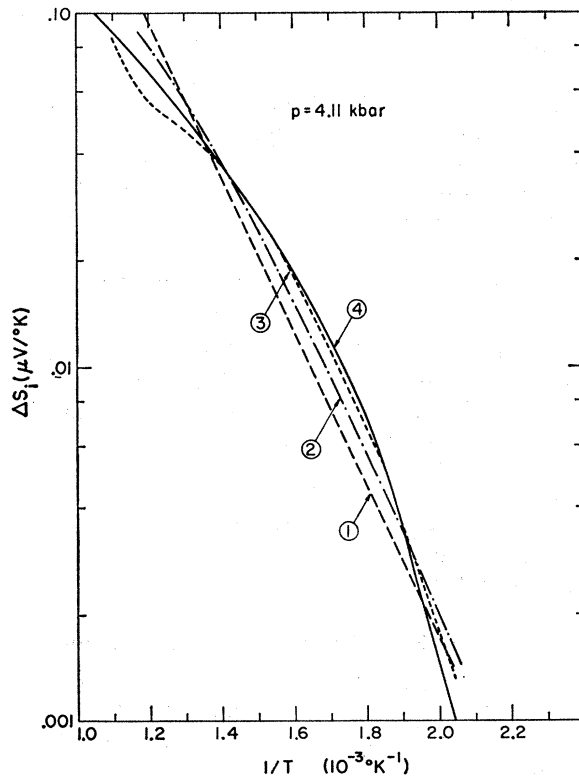


FIG. 6. Comparison of one-, two-, and three-defect models to the measured change in thermoelectric power due to defects: (1) best fit using a one-defect model; (2) best fit using a two-defect model; (3) best fit using a three-defect model; (4) measured change in thermoelectric power due to defects.

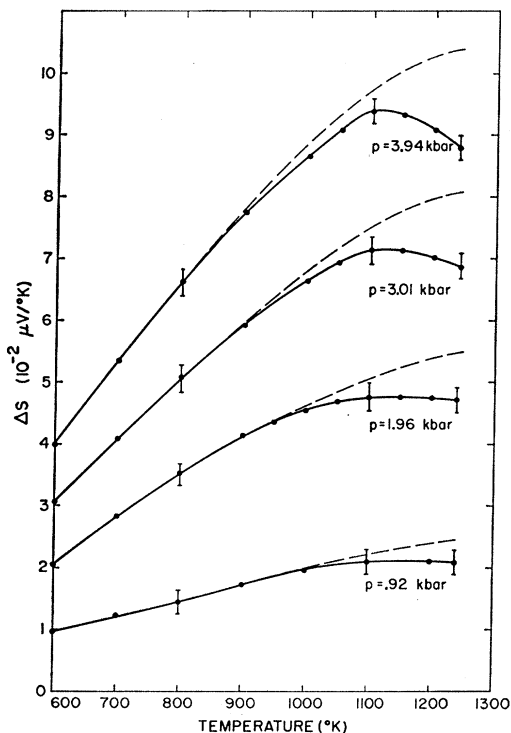


FIG. 7. Change in thermoelectric power with pressure as a function of temperature for gold. Dotted curves represent the expected result after subtraction of the vacancy effect.

Fig. 7. The values of  $\Delta U_F$  and  $\Delta S_{Th}/k$  were taken as 0.94 and 1.0 eV, respectively.<sup>8</sup> Huebener's value for  $\delta S/C$  was used. The fit is quite satisfactory.

Isotherms of  $\Delta S$  as a function of pressure, indicate that  $\Delta S$  is linear in the pressure for all temperatures.

### C. Discussion of Thermoelectric-Power Data: Nickel and Platinum

The change in the thermoelectric power of nickel and platinum with pressure as a function of temperature is shown in Fig. 8. The change in scattering mechanism at the Curie point of nickel appears as a sharp discontinuity in  $\Delta S$ .

Due to a catastrophic failure of the pressure vessel, only one run was made on platinum. As expected, no change was apparent in scattering mechanism within our temperature range.

### D. Discussion of Resistance Data: Aluminum

The pressure coefficient of resistance versus temperature for aluminum and gold is shown in Fig. 9. Low-temperature data of Bridgman<sup>15</sup> are also indicated. The pressure coefficient of resistance is independent of pressure in our pressure range within the accuracy of our data.

<sup>15</sup> P. W. Bridgman, Proc. Am. Acad. Arts Sci. 58, 151 (1923).

Assuming that the formation enthalpy  $\Delta H_F$  of a vacancy can be expanded in a Taylor series in the volume, and that  $\Delta H_F$  can be presumed to be linear in  $\theta_R$ , then

$$\Delta H_F(P_2) - \Delta H_F(P_1) = \Delta P (d \ln \theta_R / dP) \Delta H_F(P_1). \quad (47)$$

However,

$$\Delta H_F(P_2) - \Delta H_F(P_1) = \Delta P \Delta V_F. \quad (48)$$

Thus,

$$\Delta V_F = \Delta H_F(P_1) d \ln \theta_R / dP, \quad (49)$$

or, since  $P_1 \Delta V_F \ll \Delta U_F$ ,

$$\Delta V_F = \Delta U_F d \ln \theta_R / dP. \quad (50)$$

Dugdale and Gugan<sup>16</sup> describe a method to determine  $d \ln \theta_R / d \ln V$  from the pressure coefficient of resistivity. Assume that the resistivity can be written

$$\rho = (KT/M\theta_R^2) f(T/\theta_R), \quad (51)$$

where  $M$  is the ion mass,  $K$  is a measure of the electron-lattice interaction, and where we take  $f$  as an arbitrary function. Then,

$$(d \ln \rho / dP)_T = d \ln K / dP - (d \ln \theta_R / dP) [1 + (\partial \ln \rho / \partial \ln T)_P]. \quad (52)$$

The slope of  $(\partial \ln \rho / \partial P)_T$  versus  $[1 + (\partial \ln \rho / \partial \ln T)_P]$  should give  $d \ln \theta_R / dP$ , and that curve is shown for Al and Au in Fig. 10; the values for  $\rho$  as a function of  $T$

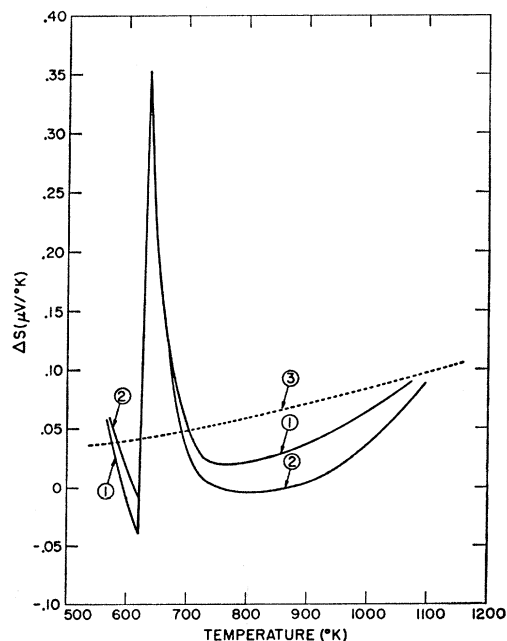


FIG. 8. Change in the thermoelectric power with pressure as a function of temperature for nickel and platinum: (1) 1-kbar nickel run; (2) 2-kbar nickel run; (3) 3-kbar platinum run.

<sup>16</sup> J. S. Dugdale and D. Gugan, Proc. Roy. Soc. (London) A241, 397 (1957).

were taken from Simmons and Balluffi,<sup>17</sup> and values of the isothermal compressibility were taken from Sutton.<sup>18</sup>

Between 600 and 700°K we find for aluminum

$$d \ln \theta_R / dP = 0.0085 \text{ kbar}^{-1}. \quad (53)$$

If we associate this region with monovacancies, Eq. (50) can be used to determine a value for the formation volume of a monovacancy. Assuming that  $\Delta U_F^1 = 0.74$  eV, we find

$$\Delta V_F^1 = 1.0 \pm 0.1 \times 10^{-23} \text{ cm}^3, \quad (54)$$

in close agreement with the result determined from the thermoelectric-power measurement.

Above 800°K we find

$$d \ln \theta_R / dP = 0.0167 \text{ kbar}^{-1}. \quad (55)$$

We interpret this doubling of  $d \ln \theta_R / dP$  as an indication that divacancies are present. If we assume that only divacancies are present and that

$$\Delta V_F^2 = (d \ln \theta_R / dP) \Delta U_F^2, \quad (56)$$

we find that for  $\Delta U_F^2 = 0.91$  eV,

$$\Delta V_F^2 = 2.4 \pm 0.3 \times 10^{-23} \text{ cm}^3. \quad (57)$$

This value is expected to be too high because there are also a large number of monovacancies present at high temperature. Thus, some fraction of  $d \ln \theta_R / dP$  should still be due to single vacancies; this result is, therefore, also consistent with the value of  $\Delta V_F^2 \approx 1.6 \times 10^{-23} \text{ cm}^3$  obtained in the thermoelectric-power measurement.

**E. Discussion of Resistance Data : Gold**

The pressure coefficient of resistance as a function of temperature for gold, shown in Fig. 9, is found to be independent of pressure in our pressure range. A value

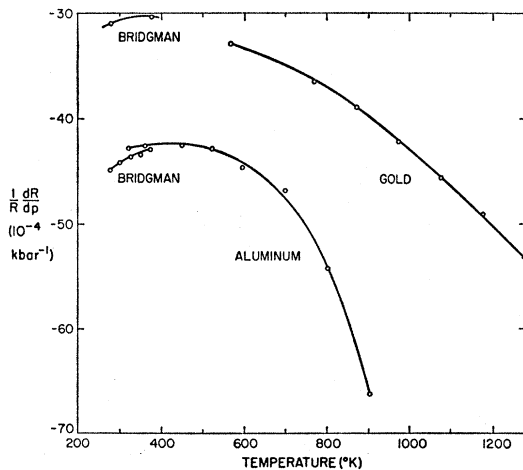


FIG. 9. The pressure coefficient of resistance as a function of temperature.

<sup>17</sup> R. O. Simmons and R. W. Balluffi, Phys. Rev. **117**, 62 (1960).  
<sup>18</sup> P. M. Sutton, Phys. Rev. **91**, 816 (1953).

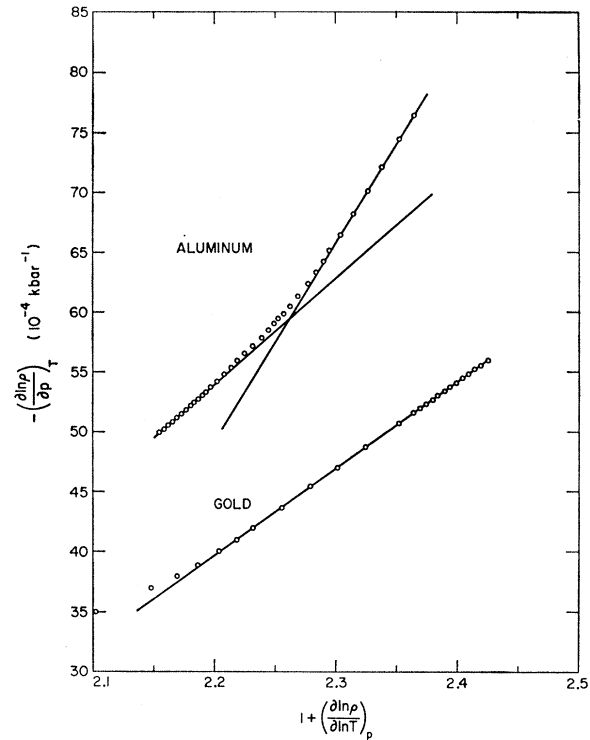


FIG. 10. The pressure coefficient of resistivity versus 1 plus the logarithmic temperature derivative of the resistivity at constant pressure.

of  $(0.916 \pm 0.068) \times 10^{-23} \text{ cm}^3$  has been reported for the formation volume in Au by Huebener and Homan<sup>19</sup> and by Grimes.<sup>20</sup>

We can test the present phenomenological model by applying Eq. (52) to Au. The graph of  $(d \ln \rho / dP)_T$  versus  $[1 + (\partial \ln \rho / \partial \ln T)_P]$  is shown in Fig. 10 and is used to determine the value

$$d \ln \theta_R / dP = 0.0072 \text{ kbar}^{-1}. \quad (58)$$

Using  $\Delta U_F = 0.94$  eV, we then find

$$\Delta V_F = (1.08 \pm 0.10) \times 10^{-23} \text{ cm}^3. \quad (59)$$

This value is consistent with the previously measured value of  $\Delta V_F$ .

**IV. SUMMARY AND CONCLUSIONS**

The temperature dependence of the change in thermoelectric power with pressure of aluminum was found to depart significantly from a single vacancy model. The departure is attributed to the presence of impurity-vacancy pairs and divacancies. Data at seven pressures and all temperatures are combined to form a pressure-

<sup>19</sup> R. P. Huebener and C. G. Homan, Phys. Rev. **129**, 1162 (1963).  
<sup>20</sup> H. H. Grimes, J. Phys. Chem. Solids **26**, 509 (1965)

temperature surface. A least-squares fit based on a three-defect model gave the following values for the formation energy and formation volume of each of the three defects:

$$\Delta U_{F^1} = 0.74 \text{ eV}, \quad (60)$$

$$\Delta V_{F^1} = 0.9 \times 10^{-23} \text{ cm}^3, \quad (61)$$

$$\Delta U_{F^2} = 0.91 \text{ eV}, \quad (62)$$

$$\Delta V_{F^2} = 1.6 \times 10^{-23} \text{ cm}^3, \quad (63)$$

$$\Delta U_{F^{iv}} = 0.64 \text{ eV}, \quad (64)$$

$$\Delta V_{F^{iv}} = 0.6 \times 10^{-23} \text{ cm}^3. \quad (65)$$

A phenomenological model is presented to interpret the high-temperature change in resistance with pressure. This model indicates that

$$\Delta U_{F^1} = 1.0 \pm 0.1 \times 10^{-23} \text{ cm}^3 \quad (66)$$

in aluminum. Strong evidence of divacancies appears,

indicating that

$$\Delta V_{F^2} < 2.4 \pm 0.3 \times 10^{-23} \text{ cm}^3. \quad (67)$$

The change in thermoelectric power with pressure in gold is due mainly to lattice effects. A vacancy effect is also present at high temperatures, and the data are consistent with a single defect model.

The pressure coefficient of resistance of gold at high temperatures can be interpreted by the same model presented for aluminum. This model gives for gold

$$\Delta V_{F^1} = 1.08 \pm 0.1 \times 10^{-23} \text{ cm}^3, \quad (68)$$

in good agreement with the accepted value of  $0.916 \pm 0.068 \times 10^{-23} \text{ cm}^3$ . There is no evidence for divacancies up to 1273°K, possibly indicating a relatively small binding energy for divacancies in gold.

Measurement of the change in thermoelectric power with pressure of nickel and platinum successfully test the sensitivity of the method for detection of changes in scattering mechanism.

## Cyclotron Resonance in Gallium

T. W. MOORE\*

*General Electric Research and Development Center, Schenectady, New York*

(Received 11 September 1967)

Azbel'-Kaner cyclotron resonance has been studied at 36 and 9 Gc/sec at 1.2°K in the three principal symmetry planes of gallium with the microwave currents both parallel and perpendicular to the applied magnetic field. The resonance signals were characterized by extreme complexity and high resolution (long relaxation times). Mass values are determined as a function of orientation of the magnetic field in the sample surfaces. No interpretation of the mass branches on a model Fermi surface is attempted, but some correlations with previous de Haas-van Alphen data are presented.

### I. INTRODUCTION

BECAUSE of its ready availability, ease of sample preparation, and extremely long electron relaxation times, gallium has become a favorite material for experimental investigations of transport phenomena in metals at low temperatures.<sup>1</sup> Despite extensive effort, the Fermi surface (FS) remains largely unknown. In contrast to nearly all other polyvalent metals,<sup>2</sup> the single orthogonalized-plane-wave (OPW) model<sup>3</sup> has not provided even a "zero-order" FS for the interpretation of experimental data. The most striking aspect of this failure is the complete absence in experimental data of the pseudohexagonal symmetry which is the most prominent feature of the single OPW model. Extensive augmented-plane-wave (APW) band cal-

culations by Wood,<sup>4</sup> "fine-grained" by most standards, have not yet led to conclusive correlations of experimental data with a model FS. The interpretation of data from various experiments is further confused by the possibility that magnetic breakdown effects are present but undetected in some experimental situations.<sup>5</sup> Documentation of the FS will probably await further band calculations which include spin-orbit coupling and an estimate of the size of the spin-orbit energy gaps.<sup>6</sup>

It is the primary purpose of this paper to present the results of effective mass determinations by means of cyclotron resonance. Phenomenological aspects of linewidths and relaxation times<sup>7</sup> and magnetic breakdown<sup>5</sup> which arose in the course of this work have been previously reported. In Sec. II some pertinent experi-

\* Present address: Department of Physics, Mount Holyoke College, South Hadley, Mass.

<sup>1</sup> A. Goldstein and S. Foner, *Phys. Rev.* **146**, 442 (1966).

<sup>2</sup> W. A. Harrison, *Phys. Rev.* **118**, 1190 (1960).

<sup>3</sup> W. A. Reed and J. A. Marcus, *Phys. Rev.* **126**, 1298 (1962).

<sup>4</sup> J. H. Wood, *Phys. Rev.* **146**, 432 (1966).

<sup>5</sup> T. W. Moore, *Phys. Rev. Letters* **18**, 310 (1967).

<sup>6</sup> G. F. Koster, *Phys. Rev.* **127**, 2044 (1962).

<sup>7</sup> T. W. Moore, *Phys. Rev. Letters* **16**, 581 (1966).